Higher Order Eigenfields in Mode II Cracks Under Elastic-Plastic Deformation

Insu Jeon, Yongwoo Lee
Graduate student, Department of Mechanical Engineering, KAIST Science Town, Taejeon 305-701, Korea
Seyoung Im*
Department of Mechanical Engineering, KAIST Science Town, Taejeon 305-701, Korea

The explicit formulation of the J-integral and the M-integral is constructed in terms of the stress intensity factor and the higher order stress coefficients for Mode II cracks under small or large scale yielding. Furthermore, the stress intensity factor and the higher order stress coefficients as well are computed with the aid of the two-state J- and the M-integral, which is found to be accurate and efficient. It is found that the contribution from the higher order singularities to the J-integral is closely related to the configuration of the plastic zone.

Key Words: Higher Order Stress Coefficients, Stress Intensity Factor, Two-State J-And M-Integral, Configuration Of The Plastic Zone

1. Introduction

Under the small scale yielding assumption, many researchers customarily disregarded the higher order singularities in the complete Williams eigenfunction expansion. More often than not, only the stress intensities of the inverse square singularity and T-stress are employed to represent the displacement and stress field near the crack tip for examining the initiation of crack growth. However, Hui and Ruina (1995) contended that if there exists a plastic zone around the crack tip, the complete solution in elastically deformed material outside the plastic zone should include the higher order singular terms. There is another work along this line. Chen and Hasebe (1997) investigated the explicit formulations of the J-integral in terms of the coefficients of the complete Williams expansion form for a semi-infinite crack with a plastic zone around the crack tip. They used the technique based on the so-called pseudo orthogonality property of the complete Williams expansion (Chen and Hasebe, 1994a, b). More practically the J-integral is employed together with crack-tip opening displacement to estimate crack deriving force for mismatched joints with interfacial cracks (Kim and Lee, 2000).

The two-state conservation integrals stem from the conservation laws for two equilibrium states and they were proposed by Eshelby (1956) and later by Chen and Shield (1997). Among these two-state conservation laws, the two-state L-integral has been employed by Choi and Earmme (1992) in relation to computing the stress intensities for circular arc-shaped cracks, and the application of the two-state M-integral has been examined by Im and Kim (2000). The two-state J-integral has been widely used for obtaining stress intensities and elastic T-stress. Kfouri (1986), Matos et al. (1989), Cho et al. (1994) and Jeon et al. (1996) used this two-state J-integral successfully to compute the stress intensity factors. For analyzing elastic-plastic cracks, Jeon and Im (2001) applied the two-state J-integral and the two-state M-integral as well.

* Corresponding Author,
E-mail : sim@mail.kaist.ac.kr
TEL : +82-42-869-3028; **FAX** : +82-42-869-3210
Department of Mechanical Engineering, KAIST Science Town, Taejeon 305-701, Korea. (Manuscript **Received** August 9, 2002; **Revised** November 15, 2002)

Furthermore, Jeon and Im (2001) investigated the role of the higher order singularities in elastic-plastic crack problems under Mode I. They showed that the J-integral and the M-integral comprise only the contributions from the mutual interaction between all complementary pairs of the eigenfields, and found that the higher order singularities interact with the nonsingular higher order eigenfields to generate the extra configurational force, in addition to the energetic force resulting from the inverse square root singularity. This additional J-value is associated with the translation of the plastic zone alone, with the crack tip being fixed.

In this paper, we utilize the two-state J-integral and the two-state M-integral for analyzing the elastic-plastic crack under Mode II deformation. Following Jeon and Im (2001), we first summarize the two-state conservation law and the complete Williams eigenfunction expansion. Next we consider SENT (the single edged notch tension) panel to examine its complete eigenfunction expansion and to discuss the significance of the higher order singularities for Mode II cracks. Numerical examples are presented for illustrating the correlation between the higher order eigenfields and the configurations of plastic zone.

2. Governing Equation and the Two-State Conservation Integral

Consider a cracked specimen as shown in Figs. 1 and 2. We restrict our attention to the plane strain problem and the origin of the coordinate is located in the crack tip (see Fig. 2). We assume that the material properties of the body are isotropic, and that some in-planar loading is applied on the far-field boundary. Then in the absence of body forces the equilibrium equation is written as

$$\sigma_{\alpha\beta,\alpha}=0 \quad (\alpha,\ \beta=1,\ 2)$$

where the comma indicates the partial differentiation with respect to the Cartesian coordinate x_i.

Near the crack tip, plastic deformation will occur when the loading on the far-field boundary increases. For the plastic zone, we select the Prandtl-Reuss equations for incremental plasticity theory of isotropic-hardening materials (McMeeking, 1977). The constitutive law is

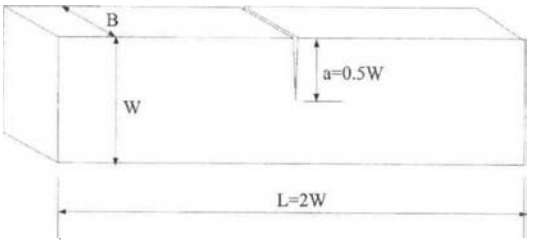

Fig. 1 The single edged notch tension (SENT) panel

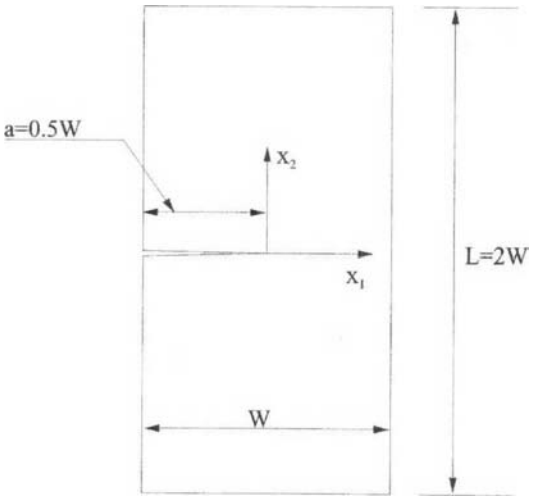

Fig. 2 The SENT panel for plane strain deformation

$$\tau_{ij}^{*}=\frac{E}{1+\nu}\left[D_{ij}+\frac{\nu}{1-2\nu}D_{kk}\delta_{ij}-\frac{3\sigma'_{ij}\sigma'_{kl}D_{kl}\left(\frac{E}{1+\nu}\right)}{2\bar{\sigma}^{2}\left(\frac{2}{3}h+\frac{E}{1+\nu}\right)}\right] \quad (1a)$$

for plastic loading and

$$\tau_{ij}^{*}=\frac{E}{1+\nu}\left[D_{ij}+\frac{\nu}{1-2\nu}D_{kk}\delta_{ij}\right] \quad (1b)$$

for elastic loading or unloading, where ν is Poisson's ratio; τ is the Kirchhoff stress defined by

$$\tau=\hat{f}\sigma$$

where $\hat{f}$ is the ratio of volume in the current state to volume in the reference state; σ is the true stress tensor; $\boldsymbol{D}$ is the rate of deformation tensor defined as the symmetric part of the spatial velocity gradient; δ_{ij} is the Kronecker delta. Furthermore, let the stress deviator σ'_{ij} and the tensile

equivalent stress $\bar{\sigma}$ be defined as

$$\sigma'_{ij}=\sigma_{ij}-\frac{1}{3}\delta_{ij}\sigma_{kk},\ \bar{\sigma}^2=\frac{3}{2}\sigma'_{ij}\sigma'_{ij} \tag{2}$$

Note that h is the slope of the uniaxial Kirchhoff stress versus logarithmic plastic strain curve, which is obtained from a given uniaxial hardening rule, and that the superscript '*' denotes the Jaumann or the co-rotational stress-rate.

For the elastic region outside the plastic zone, we assume an infinitesimal deformation behavior to which the classical linear theory of elasticity is applicable. Then we have the following constitutive equations

$$\sigma_{ij}=C_{ijkm}\varepsilon_{km},$$
$$C_{ijkm}=\mu\delta_{ik}\delta_{jm}+\mu\delta_{im}\delta_{jk}+2\nu\mu\delta_{ij}\delta_{km}/(1-2\nu) \tag{3a}$$

$$\text{with } \varepsilon_{\alpha\beta}=(u_{\alpha,\beta}+u_{\beta,\alpha})/2,\quad (\alpha,\beta=1,2) \text{ and } \varepsilon_{3\alpha}=0 \tag{3b}$$

where μ and ν are shear modulus and Poisson's ratio, respectively.

For the plane problem, the J-integral (Eshelby, 1956; Rice, 1968) and M-integral (Knowles and Sternberg, 1972) may be written as:

$$J=\int_\Gamma (Wn_1-t_iu_{i,1})\,ds \tag{4a}$$

$$M=\int_\Gamma (Wn_l-t_iu_{i,l})\,x_1 ds \tag{4b}$$

where n_l is the component of unit outward normal on the contour Γ (see Fig. 3); W and t_i indicate the strain energy density and the traction component, given as $W=C_{ijkm}\varepsilon_{ij}\varepsilon_{km}/2$ and $t_i=\sigma_{ij}n_j$. Furthermore the two-state J-integral and the two-state M-integral $J^{(A,B)}$ and $M^{(A,B)}$ (see Eshelby, 1956; Chen and Shield, 1977; Im and Kim, 2000; Jeon and Im, 2001) are given as

$$J^{(A,B)}=\int_\Gamma [C_{ijkm}\varepsilon^A_{ij}\varepsilon^B_{km}n_1-(t^A_iu^B_{i,1}+t^B_iu^A_{i,1})]\,ds \tag{5a}$$

$$M^{(A,B)}=\int_\Gamma [C_{ijkm}\varepsilon^A_{ij}\varepsilon^B_{km}n_l-(t^A_iu^B_{i,l}+t^B_iu^A_{i,l})]\,x_1 ds \tag{5b}$$

where the superscripts "A" and "B" indicate two independent elastic states "A" and "B" for the plane problem. For convenience, we rewrite $J^{(A,B)}$ and $M^{(A,B)}$ as

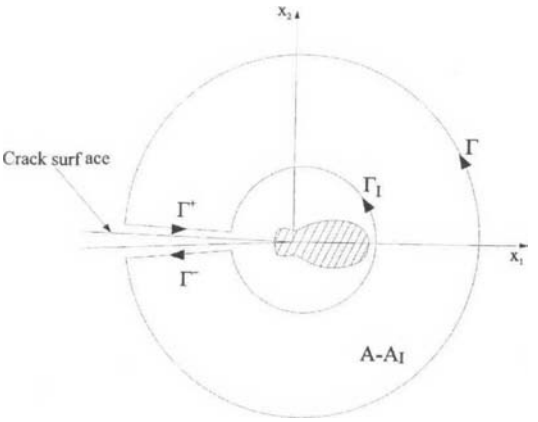

Fig. 3 The integral path for J-integral, M-integral and two-state conservation integrals

$$J^{(A,B)}=J(A,B)+J(B,A) \tag{6a}$$

$$M^{(A,B)}=M(A,B)+M(B,A) \tag{6b}$$

where $J^{(A,B)}$ and $J^{(A,B)}$ are given as

$$J(A,B)=\int_\Gamma\left(\frac{1}{2}\sigma^A_{km}\varepsilon^B_{km}n_1-t^A_iu^B_{i,1}\right)ds \tag{7a}$$

$$M(A,B)=\int_\Gamma\left(\frac{1}{2}\sigma^A_{km}\varepsilon^B_{km}n_l-t^A_iu^B_{i,l}\right)x_1 ds \tag{7b}$$

then we see that $J(A,B)\neq J(B,A)$ and $M(A,B)\neq M(B,A)$ from the Eq. (7a, b).

The two-state conservation integrals $J^{(A,B)}$ and $M^{(A,B)}$ are associated with the J- and the M-integral, respectively. They indicate the conservation integrals resulting from the mutual interaction between the two elastic states "A" and "B". The domain integral representation of $J^{(A,B)}$ and $M^{(A,B)}$ (Li et al., 1985; Im and Kim, 2000) are given as

$$J^{(A,B)}=\int_{A-A_l}[(\sigma^A_{ij}u^B_{i,1}+\sigma^B_{ij}u^A_{i,1})\,q_{,j}-\sigma^A_{km}\varepsilon^B_{km}q_{,1}]\,dA \tag{8a}$$

$$M^{(A,B)}=\int_{A-A_l}[(\sigma^A_{ij}u^B_{i,1}+\sigma^B_{ij}u^A_{i,1})\,x_1q_{,j}-\sigma^A_{km}\varepsilon^B_{km}x_1q_{,1}]\,dA \tag{8b}$$

3. The Application of the Two-State Conservation Integral to Mode II Elastic-Plastic Cracks

Consider a mode II crack under elastic-plastic deformation around the crack tip. We take the origin of the coordinate system at the crack tip (see Fig. 2). Let $R\neq 0$ denote the maximum

radius of the plastic zone, i.e., the length of the maximum radial distance from the crack tip to the elastic-plastic boundary. The stress and displacement field for the Mode II deformation may be obtained using the stress potential of Timoshenko and Goodier (1987). The complete Williams eigenfunction expansion of the Laurent series type for mode II crack in the presence of the plastic zone (Dickerson and Kim, 1988) are given as:

$$\sigma_{11}=\frac{K_{II}}{\sqrt{2\pi R}}\{\sum_{n=-\infty}^{\infty}\beta_n\hat{r}^{\delta_n}[(2-C_n(\delta_n+2))(\delta_n+1)\sin\delta_n\theta-\delta_n(\delta_n+1)\sin(\delta_n-2)\theta]\} \quad (9a)$$

$$\sigma_{22}=\frac{K_{II}}{\sqrt{2\pi R}}\{\sum_{n=-\infty}^{\infty}\beta_n\hat{r}^{\delta_n}[(2+C_n(\delta_n+2))(\delta_n+1)\sin\delta_n\theta+\delta_n(\delta_n+1)\sin(\delta_n-2)\theta]\} \quad (9b)$$

$$\sigma_{12}=\frac{K_{II}}{\sqrt{2\pi R}}\{\sum_{n=-\infty}^{\infty}\beta_n\hat{r}^{\delta_n}[(-)C_n(\delta_n+1)(\delta_n+2)\cos\delta_n\theta-\delta_n(\delta_n+1)\cos(\delta_n-2)\theta]\} \quad (9c)$$

$$\sigma_{33}=\nu(\sigma_{11}+\sigma_{22}),\ \sigma_{13}=\sigma_{23}=0 \quad (9d)$$

$$u_1=\frac{K_{II}\sqrt{R}}{2\mu\sqrt{2\pi}}\{\sum_{n=-\infty}^{\infty}\beta_n\hat{r}^{\delta_n+1}[(\kappa-C_n(\delta_n+2))\sin(\delta_n+1)\theta-(\delta_n+1)\sin(\delta_n-1)\theta]\} \quad (9e)$$

$$u_2=\frac{K_{II}\sqrt{R}}{2\mu\sqrt{2\pi}}\{\sum_{n=-\infty}^{\infty}\beta_n\hat{r}^{\delta_n+1}[(-)(\kappa-C_n(\delta_n+2))\cos(\delta_n+1)\theta-(\delta_n+1)\cos(\delta_n-1)\theta]\} \quad (9f)$$

where $\hat{r}=\frac{r}{R}>1$ and the eigenvalues δ_n are given as Λ, $\delta_{-2}=-3/2$, $\delta_{-1}=-1$, $\delta_0=-1/2$, $\delta_1=0$, $\delta_2=1/2$, Λ (see Table 2 or 3); C_n is the function of δ_n, written as

$$C_n=(-)[\sin\delta_n\pi/\sin(\delta_n+2)\pi]\quad(\delta_n=\Lambda,\ -1/2,\ 1/2,\ \Lambda)$$

$$C_n=(-)[\delta_n\cos\delta_n\pi/(\delta_n+2)\cos(\delta_n+2)\pi]\quad(\delta_n=\Lambda,\ -1,\ 0,\ 1,\ \Lambda)$$

The stress coefficient β_n is related to the eigenvalue δ_n. Note that β_0, which is set to '1' for convenience, is the coefficient of the eigenvalue $\delta_0=-1/2$ for Mode II and that $K_{II}\beta_0=K_{II}$ is the stress intensity factor.

For crack problems under Mode II, wherein $J^{(A,B)}$ and $M^{(A,B)}$ retain the path independence, we define the complementary pairs of eigenvalues δ_n and δ_n^c following Im and Kim (2000) and Jeo n and Im (2001) as follows:

$$\delta_n+\delta_n^c=-1:\ \textit{in the J-integral sense} \quad (10a)$$

$$\delta_n+\delta_n^c=-2:\ \textit{in the M-integral sense} \quad (10b)$$

For an arbitrary eigenvalue δ_n, we have the complementary eigenvalue $\delta_n^c=-1-\delta_n$ in the J-integral sense and $\delta_n^c=-2-\delta_n$ in the M-integral sense, respectively. Furthermore for cracks, we may verify that both of $\delta_n^c=-1-\delta_n$ and $\delta_n^c=-2-\delta_n$ are also eigenvalues whenever δ_n is an eigenvalue.

Consider an eigenfield corresponding to an arbitrary eigenvalue δ_n^c. We define this field to be an auxiliary elastic state, which is to be utilized for the state "B" in the two-state integrals (5a, b). It may be obtained by taking only the eigenfunction term corresponding to the eigenvalue δ_n^c in the expressions (9a-f):

$$\sigma_{11}(\delta_n^c)=\frac{K_{II}^c}{\sqrt{2\pi R}}\beta_n^c\hat{r}^{\delta_n^c}[(2-C_n^c(\delta_n^c+2))(\delta_n^c+1)\sin\delta_n^c\theta-\delta_n^c(\delta_n^c+1)\sin(\delta_n^c-2)\theta] \quad (11a)$$

$$\sigma_{22}(\delta_n^c)=\frac{K_{II}^c}{\sqrt{2\pi R}}\beta_n^c\hat{r}^{\delta_n^c}[(2+C_n^c(\delta_n^c+2))(\delta_n^c+1)\sin\delta_n^c\theta+\delta_n^c(\delta_n^c+1)\sin(\delta_n^c-2)\theta] \quad (11b)$$

$$\sigma_{12}(\delta_n^c)=\frac{K_{II}^c}{\sqrt{2\pi R}}\beta_n^c\hat{r}^{\delta_n^c}[(-)C_n^c(\delta_n^c+1)(\delta_n^c+2)\cos\delta_n^c\theta-\delta_n^c(\delta_n^c+1)\cos(\delta_n^c-2)\theta] \quad (11c)$$

$$\sigma_{33}(\delta_n^c)=\nu(\sigma_{11}(\delta_n^c)+\sigma_{22}(\delta_n^c)),\ \sigma_{13}(\delta_n^c)=\sigma_{23}(\delta_n^c)=0 \quad (11d)$$

$$u_1(\delta_n^c)=\frac{K_{II}^c\sqrt{R}}{2\mu\sqrt{2\pi}}\beta_n^c\hat{r}^{\delta_n^c+1}[(\kappa-C_n^c(\delta_n^c+2))\sin(\delta_n^c+1)\theta-(\delta_n^c+1)\sin(\delta_n^c-1)\theta] \quad (11e)$$

$$u_2(\delta_n^c)=\frac{K_{II}^c\sqrt{R}}{2\mu\sqrt{2\pi}}\beta_n^c\hat{r}^{\delta_n^c+1}[(-)(\kappa+C_n^c(\delta_n^c+2))\cos(\delta_n^c+1)\theta-(\delta_n^c+1)\cos(\delta_n^c-1)\theta] \quad (11f)$$

where β_n^c is the stress coefficient for the complementary eigenfunction and K_{II}^c is the stress intensity factor of the complementary eigenfield when β_0^c being defined to be 1. Here C_n^c is the function of δ_n^c, written as

$$C_n^c=(-)[\sin\delta_n^c\pi/\sin(\delta_n^c+2)\pi]\quad(\delta_n^c=\Lambda,\ -1/2,\ 1/2,\ \Lambda)$$

$$C_n^c=(-)[\delta_n^c\cos\delta_n^c\pi/(\delta_n^c+2)\cos(\delta_n^c+2)\pi]\quad(\delta_n^c=\Lambda,\ -1,\ 0,\ 1,\ \Lambda)$$

We now consider the superposition of this auxiliary elastic state onto the given elastic state outside the plastic zone for an elastic-plastic

crack problem under consideration. For the elastic state "A" we substitute the elastic field (9a-f), which has been obtained by replacing the plastic zone by the elastic singularities, and the auxiliary field (11a-f) for the elastic state "B". We reach the following expression for $J^{(A,B)}$ and $M^{(A,B)}$ of Eq. (5a, b) after some algebra:

$$J^{(A,B)}=\sum_{k=-\infty}^{\infty} J^{(\delta_k,\delta_n^c)} \text{ and } M^{(A,B)}=\sum_{k=-\infty}^{\infty} M^{(\delta_k,\delta_n^c)}$$

where

$$J^{(\delta_k,\delta_n^c)}=\int_\Gamma \frac{K_I K_I^c}{2\pi R}\beta_k\beta_n^c \hat{r}^{\delta_k+\delta_n^c+1}F(\delta_k,\ \delta_n^c,\ \theta)\,d\theta$$

$$M^{(\delta_m,\delta_n^c)}=\int_\Gamma \frac{K_I K_I^c}{2\pi R}\beta_m\beta_n^c \hat{r}^{\delta_m+\delta_n^c+2}G(\delta_m,\ \delta_n^c,\ \theta)\,d\theta$$

and Γ is a circuit enclosing the plastic zone. Note that $F(\delta_k,\ \delta_n^c,\ \theta)$ and $G(\delta_m,\ \delta_n^c,\ \theta)$ are functions which are independent of the "r"-coordinate. They depend only upon the eigenvalues and "θ" -coordinate. We exploit the path-independence characteristics of $J^{(\delta_k,\delta_n^c)}$ and $M^{(\delta_m,\delta_n^c)}$ to show that the contributions of all δ_k and δ_m to the two-state conservation integrals vanish identically except for $\delta_k=-1-\delta_n^c=\delta_n$ in $J^{(\delta_k,\delta_n^c)}$ and $\delta_m=-2-\delta_n^c=\delta_n$ in $M^{(\delta_m,\delta_n^c)}$. That is, we take $\hat{r}$ to go to infinity for $\delta_k+\delta_n^c<-1$ in $J^{(\delta_k,\delta_n^c)}$ and for $\delta_m+\delta_n^c<-2$ in $M^{(\delta_m,\delta_n^c)}$ while we take $\hat{r}$ to be arbitrarily small for each of $\delta_k+\delta_n^c\geq -1$ and $\delta_m+\delta_n^c\geq -2$ (see Im and Kim, 2000). Hence we have

$$J^{(\delta_k,\delta_n^c)}=0 \text{ or } \int_\Gamma F(\delta_k,\ \delta_n^c,\ \theta)\,d\theta=0 \quad \text{unless } \delta_k=-1-\delta_n^c \tag{12a}$$

$$M^{(\delta_m,\delta_n^c)}=0 \text{ or } \int_\Gamma G(\delta_m,\ \delta_n^c,\ \theta)\,d\theta=0 \quad \text{unless } \delta_m=-2-\delta_n^c \tag{12b}$$

Hence the mutual interaction integrals or the two-state integrals $J^{(\delta_p,\delta_q)}$ and $M^{(\delta_s,\delta_q)}$ vanish unless the two eigenvalues are complementary to each other. It follows from this that

$$J^{(A,B)}=J^{(\delta_n,\delta_n^c)}$$
$$M^{(A,B)}=M^{(\delta_n,\delta_n^c)}$$

Now we calculate these two-state integrals with the aid of Eqs. (5a, b), (9a-f) and (11a-f), finally to reach

$$J^{(A,B)}=(-)\frac{K_{II}K_{II}^c}{2\mu}(\kappa+1)\beta_n\beta_n^c[C_n(\delta_n+1)(\delta_n+2)(\delta_n^c+1)+C_n^c(\delta_n^c+1)(\delta_n^c+2)(\delta_n+1)+(\delta_n+1)(\delta_n^c+1)] \quad (\text{for } n=-\infty,\ \Lambda,\ -1,\ 0,\ 1,\ \Lambda,\ \infty) \tag{13a}$$

$$M^{(A,B)}=(-)\frac{K_{II}K_{II}^c}{2\mu}R(\kappa+1)\beta_n\beta_n^c[C_n(\delta_n+1)(\delta_n+2)(\delta_n^c+1)+C_n^c(\delta_n^c+1)(\delta_n^c+2)(\delta_n+1)] \quad (\text{for } n=-\infty,\ \Lambda,\ -1,\ 0,\ 1,\ \Lambda,\ \infty) \tag{13b}$$

Take $K_{II}^c\,\beta_n^c=1$ for convenience to compute $J^{(A,B)}$ and $M^{(A,B)}$ in (13a, b). We compute the left hand side of Eq. (13a, b) by applying Eq. (8a, b) to the two states: one is the elastic state outside the plastic zone under consideration and the other is the auxiliary state or the eigenstate of the eigenvalue δ_n^c with $K_{II}^c\,\beta_n^c=1$. We then see that Eq. (13a) or (13b) provides a linear equation in $K_{II}\,\beta_n$ for each eigenvalue δ_n. The accurate computation of the two-state conservation integrals $J^{(A,B)}$ and $M^{(A,B)}$ is possible just via a regular displacement based FEM in conjunction with the domain integral representations (8a, b). In the present study, we rely upon ABAQUS for computing this finite element solution. Then the Eq. (13a) or (13b) yields $K_{II}\beta_n$ for each δ_n, that is, the stress intensity factor and the higher order stress coefficients.

According to Eq. (7a, b), $J(A,\ B)$ and $M(A,\ B)$ for the mode II are given as

$$J(\delta_n,\ \delta_n^c)=(-)\frac{K_{II}K_{II}^c}{4\mu}\beta_n\beta_n^c[2C_n\kappa(\delta_n+1)(\delta_n+2)(\delta_n^c+1)+2C_n^c(\delta_n^c+1)(\delta_n^c+2)(\delta_n+1)+(\kappa+1)(\delta_n+1)(\delta_n^c+1)] \quad (n=-\infty,\ \Lambda,\ -1,\ 0,\ 1,\ \Lambda,\ \infty) \tag{14a}$$

$$M(\delta_n,\ \delta_n^c)=(-)\frac{K_{II}K_{II}^c}{2\mu}R\beta_n\beta_n^c[C_n\kappa(\delta_n+1)(\delta_n+2)(\delta_n^c+1)+C_n^c(\delta_n^c+1)(\delta_n^c+2)(\delta_n+1)] \quad (n=-\infty,\ \Lambda,\ -1,\ 0,\ 1,\ \Lambda,\ \infty) \tag{14b}$$

As discussed before, $J(A,\ B)$ and $M(A,\ B)$ do not satisfy the path-independence property in general, but $J(A,\ B)$ becomes path-independent if "A" and "B" represent two eigenstates that are complimentary to each other in the J-integral sense (see Jeon and Im, 2001). The same applies to $M(A,\ B)$, and so we have the path-independent expressions (14a, b).

Let $J^{(\delta_n,\delta_n^c)}$ and $M^{(\delta_n,\delta_n^c)}$ indicate the mutual interaction for two eigenfields of eigenvalues δ_n

and δ_n^c. For definiteness we take $\delta_n (n=0, -1, -2, \Lambda)$ to be the eigenvalues of the singular eigenfield, i.e., $\delta_0=-1/2$, $\delta_{-1}=-1$, $\delta_{-2}=-3/2$, Λ and δ_n^c to be given by $-1-\delta_n$ for $J^{(\delta_n,\delta_n^c)}$ and by $-2-\delta_n$ for $M^{(\delta_n,\delta_n^c)}$. Relying upon the path independence of the two-state J-integral of equation (5a) and the two-state M-integral of Eq. (5b), and substituting the eigenfunction solution (9a-f) into the expressions (4a, b), we can show that the J-integral and the M-integral are nothing but the summation of the contribution from each complementary pair of eigenvalues and can be written as (see Jeon and Im, 2001)

$$J=J_0+\sum_{n=-1}^{-\infty} J^{(\delta_n,\delta_n^c)} \tag{15a}$$

$$M=M(-1, -1)+\sum_{n=-2}^{-\infty} M^{(\delta_n,\delta_n^c)} \tag{15b}$$

where $J_0=J(-1/2, -1/2)$ is the classical expression of the J-integral for elastic crack problem, calculated with the eigenvalue $\delta_0=-1/2$ alone. Furthermore J_0 associated with $\beta_0=1$ and $\beta_0^c=1$, can be obtained from Eq. (14a);

$$J_0=J(-1/2, -1/2)=\frac{(\kappa+1)K_{II}^2}{8\mu}$$

where K_{II} is a stress intensity factor for Mode II. Therefore J_0 is the same as the well-known energy release rate "G" for a Mode II elastic crack with the intensity factor K_{II}.

We assume that there are no concentrated line loads or dislocations at the crack tip. Then there appear no logarithmic terms for $\delta_{-1}=-1$, and the eigenvalue $\delta_{-1}=-1$ is related only to a rigid body mode. Therefore the first term $M(-1, -1)$ disappears in the summation (15b). Equations (15a, b) imply that the contribution to J and M by the eigenfunction of an eigenvalue δ_n is generated from the mutual interaction between this eigenfield and its complementary eigenfield. No interactions occur between two eigenfields in terms of J and M unless they are complementary to each other. For $\delta_0=-1/2$, the K_I field itself becomes its complementary field, and we have $J_0=J(-1/2, -1/2)=\frac{1}{2}J^{(-1/2,-1/2)}$. In passing, it is evident that rigid body modes should be excluded from the complementarity consideration in the view of the energy release rate.

The expressions $\sum_{n=-1}^{-\infty} J^{(\delta_n,\delta_n^c)}$ and $\sum_{n=-2}^{-\infty} M^{(\delta_n,\delta_n^c)}$ indicate the summation of the J-integral and the M-integral contributions due to the eigenvalues δ_n and their complementary eigenvalues δ_n^c. From the results of Jeon and Im (2001), we see that the term $\sum_{n=-1}^{-\infty} J^{(\delta_n,\delta_n^c)}$, associated with translation of the higher order singularities, means the energetic force with respect to the translation of the plastic zone while the crack tip being fixed. Furthermore the M-integral summation $\sum_{n=-2}^{-\infty} M^{(\delta_n,\delta_n^c)}$ may be interpreted as the energy release rate associated with the uniform expansion of the plastic zone.

4. Numerical Examples and Discussion

The numerical calculation is carried out for a material with $W=1$ m, $E=71$ GPa, $\nu=0.33$ and $\sigma_Y=303$ MPa where σ_Y is the uniaxial yield stress. For the model of this study, we select a single edge notched tension (SENT) panel (see Fig. 1 and Fig. 2), and the distributed loading are applied on the boundary of the model. Furthermore the calculation was processed with a power-law hardening material in a uniaxial stress-strain law :

$$\frac{\bar{\varepsilon}^p}{\varepsilon_Y}=\alpha\left(\frac{\bar{\sigma}}{\sigma_Y}\right)^m \tag{16}$$

Here $\bar{\varepsilon}^p$ is the plastic equivalent strain, and $\varepsilon_Y=\sigma_Y/E$ is a reference strain component ; $\bar{\sigma}$ is the Mises stress, α a nondimensional material constant, m the power-law hardening exponent. Typically $m=1$ is linear elastic and $m=\infty$ is the perfectly plastic. We choose $m=5$, 10 and ∞ as the power-law hardening exponents.

The package code ABAQUS is employed for the finite element solution, and the isoparametric plane strain elements with eight nodes (CPE8 element) are used. We select the reduced integration element to prevent the excessive incompressibility constraint due to plastic deformation. Figures 4 and 5 show the boundary condition and finite element mesh under Mode II loading. We

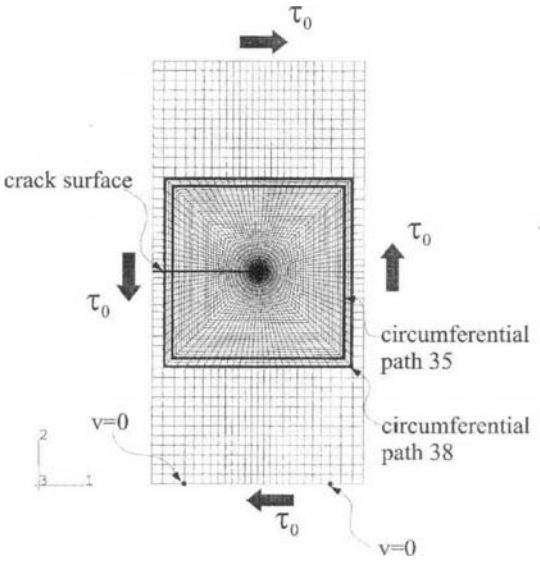

Fig. 4 The finite element mesh and boundary condition under Mode II

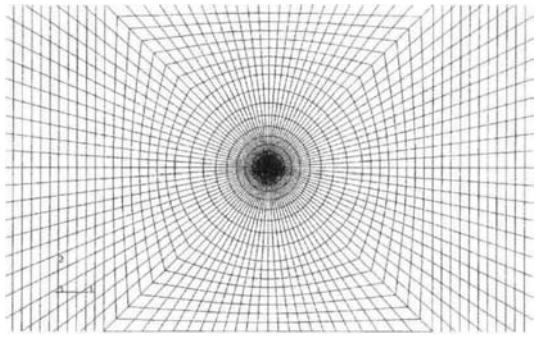

Fig. 5 The zoomed mesh near the crack tip

impose constant shear traction τ_0 along each of the four edges of the plane strain block, and the vertical degree of freedom is constrained at the two nodal points as shown in Fig. 4 to remove rigid body mode. The horizontal rigid displacement is removed by fixing a horizontal displacement to be zero on one of the bottom nodes (with its prescribed traction being replaced by the unknown reaction force). Then the vertical reactions turn out to be negligibly small and the horizontal equilibrium assures the skew-symmetric loading. The total number of elements amounts to 4228 for the small scale yielding, and to 4320 for the large scale yielding.

For the analysis of the small scale yielding

Table 1 The maximum radius of the plastic zone for Mode II for and $\tau_0/\sigma_Y=0.1$ and $\tau_0/\sigma_Y=0.31$

The maximum radius of the plastic zone size for the small and the large scale yielding	
$\tau_0/\sigma_Y=0.1$	$\tau_0/\sigma_Y=0.31$
.19529585E-01	.44538946E+00

Table 2 The calculated stress intensity factor and the higher order stress coefficients for Mode II ($m=10$, $\tau_0/\sigma_Y=0.1$)

n	δ_n	Stress coefficients (K_{II}=.47619750E+08)	
		Two state J-integral method	Two state M-integral method
5	2.0	−.65243891E−05	−.65243891E−05
4	1.5	.17035200E−04	.17035200E−04
3	1.0	*	.76000303E−03
2	0.5	.68115670E−02	.68115670E−02
0	−0.5	.10000000E−01	.10000000E−01
−2	−1.5	−.25285028E−00	−.25285028E−00
−3	−2.0	.00000000E+00	.00000000E+00
−4	−2.5	−.35873109E−01	−.35873110E+01
−5	−3.0	−.30574400E−02	−.30574435E+02

* : not computed with this method
-Rigid body translation is excluded in this table

problem we take $m=10$ and $\tau_0/\sigma_Y=0.1$. Because there are no ways to find a priori whether or not this loading state may produce the small scale yielding for Mode II, we consider the computed maximum radius of plastic zone from this analysis. In Table 1, we see that the maximum radius of plastic zone under the loading is very small compared with the dimensions of the specimen. Therefore we conclude that this corresponds to the small scale yielding. The maximum radius of plastic zone when $m=10$ and $\tau_0/\sigma_Y=0.31$ is also shown in Table 1. From the value of the maximum radius of plastic zone comparable to the dimensions of the specimen under this loading $\tau_0/\sigma_Y=0.31$, we see that this is a case of large scale yielding, which is before the specimen reaches a fully plastic state.

Table 2 and 3 show the resulting stress coefficients for the small scale yielding and the large scale yielding, utilizing the two-state J-integral

Table 3 The calculated stress intensity factor and the higher order stress coefficients for Mode II ($m=10$, $\tau_0/\sigma_Y=0.31$)

n	δ_n	Stress coefficients (K_{II}=.47619750E+08)	
		Two state J-integral method	Two state M-integral method
5	2.0	.23321117E−02	.23321117E−02
4	1.5	.23074229E−01	.23074229E−01
3	1.0	*	.92884084E−01
2	0.5	.16111483E−00	.16111483E−00
0	−0.5	.10000000E−01	.10000000E−01
−2	−1.5	−.22151578E−00	−.22151578E−00
−3	−2.0	.00000000E−00	.00000000E−00
−4	−2.5	−.37046697E−01	.37046697E−01
−4	−3.0	.11119703E−01	.11119703E−02

* : not computed with this method
-Rigid body translation is excluded in this table

and the two-state M-integral respectively. We see from Table 2 and 3 that the results from each of two-state conservation integrals are in an excellent agreement with each other. Furthermore we find that the stress coefficients related to the negative eigenvalues slightly change from small scale yielding to large scale yielding, however the coefficients associated with positive eigenvalues change rapidly from small scale yielding to large scale yielding. This is due to the nature of the normalization of the radial coordinate. We now assume that there exist no net forces on the contour surrounding the crack tip nor a dislocation at the crack tip. In Mode II, then the eigenvalue $\delta_{-1}=-1$ indicates the solution for rigid body translation along the x_2-direction and the eigenvalue $\delta_1=0$ indicates the solution for rigid body rotation (see Eq. (9a-f)). Particularly, the eigenvalue $\delta_{-3}=-2$ leads to the "*null*" elastic state, which yields identically zero displacement and zero stress. Hence we do not compute the coefficient of the eigenvalue $\delta_3=1$ using the two-state J-integral in this example. For an auxiliary field for $\delta_3=1$, we may use the solution for the center of rotation at a crack tip. For simplicity, however, we employ the two-state M-integral to calculate the coefficient of eigenvalue $\delta_3=1$.

The numerical results of the two-state J-integral using Eq. (13a) for various eigenvalues δ_n including the higher order singularities in each of the small scale yielding and the large scale yielding are tabulated in Table 4 and 5. As seen from Table 4, the contributions of the higher order singularities to J-integral are very small. This result explains that the effect of the higher order singularities on the J-integral is negligible when the small-scale yielding zone is localized near the crack tip. However when the plastic zone grows larger and larger as the applied loading increases, we see that the effect of the higher order singularities on J-integral is not negligible from Table 5. In Table 5, it shows that the contribution percentage of the higher order singularities to the J-integral is 16.32% when a total of 44 eigenvalues are taken. The computed two-state M-integrals using the Eq. (12b) are provided in Table 6 and 7. From Table 6 and 7, we see that the values of two-state M-integral increase rap-

Table 4 The two-state J-integrals associated with the higher order singularities for Mode II ($m=10$, $\tau_0/\sigma_Y=0.1$)

δ_n, δ_n^c	$J^{(\delta_n,\delta_n^c)}$	$\lvert J^{(\delta_n,\delta_n^c)}/J \rvert$ J=.28755097E+05
−0.5, −0.5	.56920971E+05	.19795089E+01
0.5, −1.5	.29410610E+03	.10227964E+01
1.0, −2.0	.00000000E+00	.00000000E+00
1.5, −2.5	.52177085E+00	.18145335E+04
2.0, −3.0	.27250931E+01	.94769045E+06

-Rigid body translation is excluded in this table.
$-J^{(-1/2,-1/2)}=2J_0$

Table 5 The two-state J-integrals associated with the higher order singularities for Mode II ($m=10$, $\tau_0/\sigma_Y=0.31$)

δ_n, δ_n^c	$J^{(\delta_n,\delta_n^c)}$	$\lvert J^{(\delta_n,\delta_n^c)}/J \rvert$ J=.52779857E+06
−0.5, −0.5	.88328370E+06	.16735243E+01
0.5, −0.5	.94571798E+05	.17918161E+00
1.0, −2.0	.00000000E+00	.00000000E+00
1.5, −2.5	.11325781E+05	.21458530E+01
2.0, −3.0	−.54973576E+02	.10415636E+03

-Rigid body translation is excluded in this table.
$-J^{(-1/2,-1/2)}=2J_0$

Table 6 The two-state M-integrals associated with the higher order singularities for Mode II (m=10, τ_0/σ_Y=0.1)

δ_n, δ_n^c	$J^{(\delta_n,\delta_n^c)}$	$\lvert M^{(\delta_n,\delta_n^c)}/M \rvert$ M=.28348691E+03
−0.5, −1.5	.28107923E+03	.99150690E+00
0.0, −2.0	.00000000E+03	.00000000E+00
0.5, −2.5	.24446905E+01	.86236449E+02
1.0, −3.0	−.41329396E+01	.14578943E+03
1.5, −3.5	.54509789E+02	.19228326E+04
2.0, −4.0	.45497240E+03	.16049150E+05

-Rigid body translation is excluded in this table.

Table 7 The two-state M-integrals associated with the higher order singularities for Mode II (m=10, τ_0/σ_Y=0.31)

δ_n, δ_n^c	$J^{(\delta_n,\delta_n^c)}$	$\lvert M^{(\delta_n,\delta_n^c)}/M \rvert$ M=.10313821E+06
−0.5, −1.5	.87145079E+05	.84493497E+00
−0.5, −1.5	.00000000E+00	.00000000E+00
−0.5, −1.5	.21133222E+05	.20490197E+00
−0.5, −1.5	−.65011872E+03	.63033742E+02
−0.5, −1.5	.32756126E+04	.31759449E+01
−0.5, −1.5	−.39864010E+02	.36711914E+03

-Rigid body translation is excluded in this table.

idly from small scale yielding to large scale yielding. This may be explained in the same way as in mode I crack [Jeon and Im, 2001]. That is, the M-integral is the energy release rate associated with the expansion of the inhomogeneity and so it is related to the size of the plastic zone. On the other hand, $J-J_0=\sum_{n=-1}^{\infty} J^{(\delta_n,\delta_n^c)}$ is the energy release rate associated with translation of the inhomogeneity, and so it is related to the overall configuration of the specimen including the inhomogeneity of plastic deformation, the geometry of the exterior boundary and the applied loading.

Figure 6 through 9 show J, J^* and J_0, and M, M^* and $M^{(-1/2,-3/2)}$ as well along the circumferential paths outside the plastic zone for the small scale and the large scale yielding. Note that J^* and M^* are the J-integral and the M-integral, respectively obtained from the domain integral representation of Eq. (8a) and (8b) with the

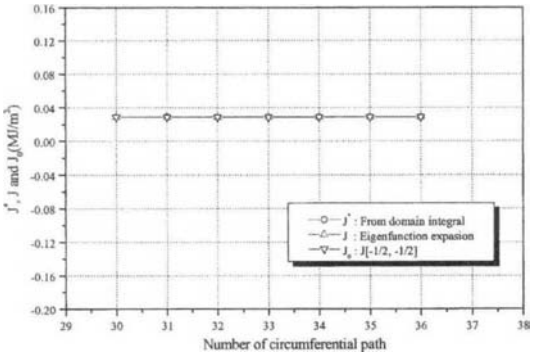

Fig. 6 The computed J-integrals along the circumferential path for Mode II (m=10, τ_0/σ_Y=0.1)

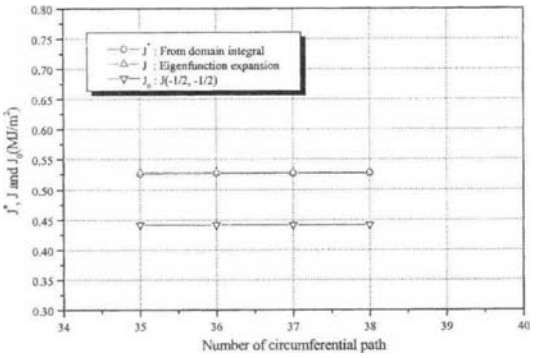

Fig. 7 The computed J-integrals along the circumferential path for Mode II (m=10, τ_0/σ_Y=0.31)

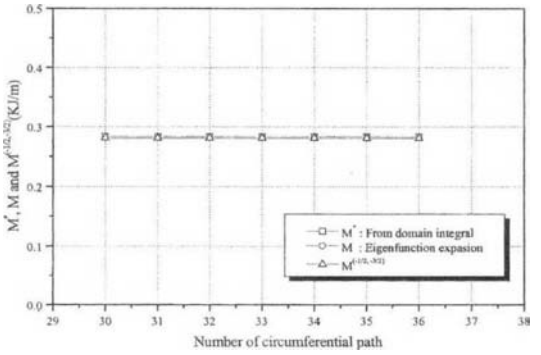

Fig. 8 The computed M-integrals along the circumferential path for Mode II (m=10, τ_0/σ_Y=0.1)

stress and the displacement gradient computed from ABAQUS. The domain integral paths for calculating J^* and M^* are shown in Fig. 4. On

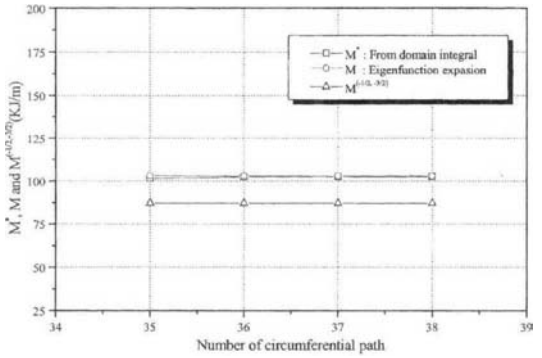

Fig. 9 The computed M-integrals along the circumferential path for Mode II ($m=10$, $\tau_0/\sigma_Y=0.31$)

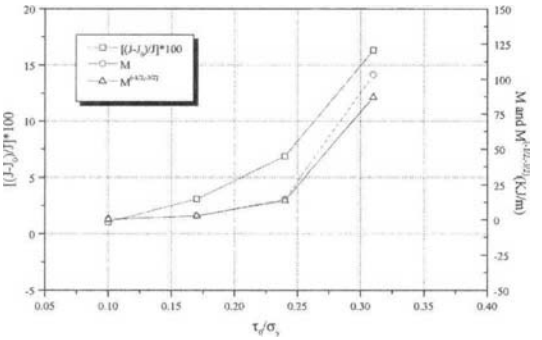

Fig. 10 The contribution perentage of the higher order singularities to J-integral and the M and $M^{(-1/2,-3/2)}$ versus the applied Mode II loading

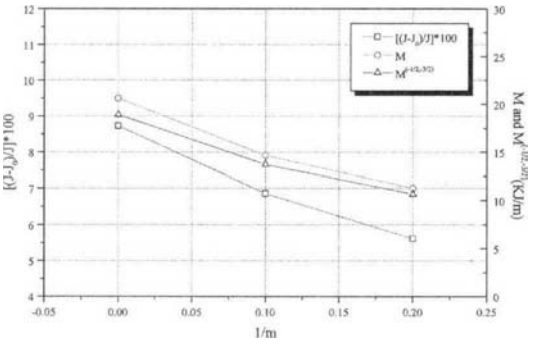

Fig. 11 The contribution perentage of the higher order singularities to J-integral and the M and $M^{(-1/2,-3/2)}$ versus the hardening exponents under Mode II

the other hand, the values of J and M are calculated from Eq. (13a, b) through (15a, b). From

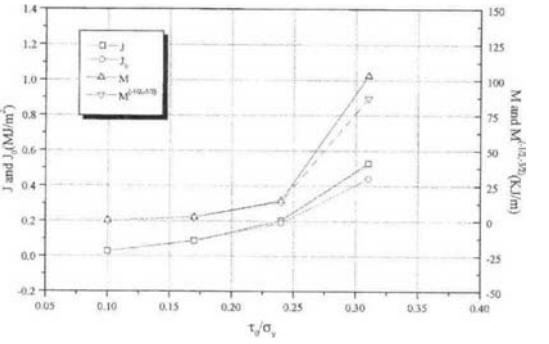

Fig. 12 The J and J_0, and M and $M^{(-1/2,-3/2)}$ versus the applied Mode II loading

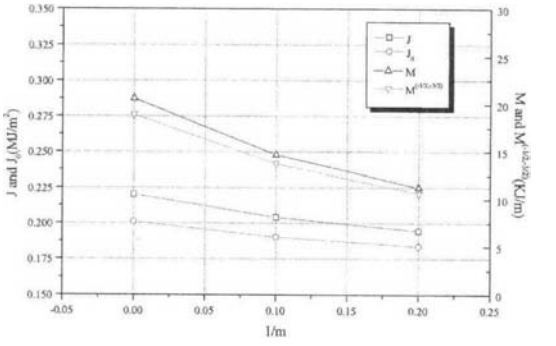

Fig. 13 The J and J_0, and M and $M^{(-1/2,-3/2)}$ versus the hardening exponents under Mode II

these figures, we see that J^* and M^* coincide with J and M within the accuracy of the FEM solution for each of the small scale and the large scale yielding. Furthermore these figures apparently show the path independence of the six integrals. The difference between J_0 and J in Fig. 7 is seen from the results of Table 5 for the large scale yielding, and the difference between $M^{(-1/2,-3/2)}$ and M in Fig. 9 means that there exist other meaningful components of $M^{(\delta_n,\delta_n^c)}$, in addition to $M^{(-1/2,-3/2)}$, that comprise the M-integral for the large scale yielding.

The contribution percentage of the higher order singularities to the J-integral in this example, $[(J-J_0)/J]*100$, and the M-integral and $M^{(-1/2,-3/2)}$ as well as the J-integral and J_0, depending upon the applied loading and the power-law hardening exponents, are plotted in Fig. 10 through 13. We obtain a rapidly increasing contribution percentage of the higher order

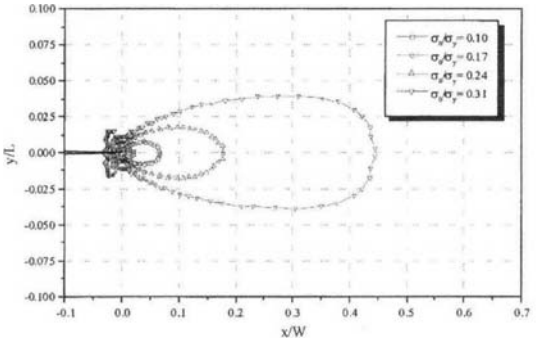

Fig. 14 The change of the plastic zone size for the various applied loading under Mode II (m=10)

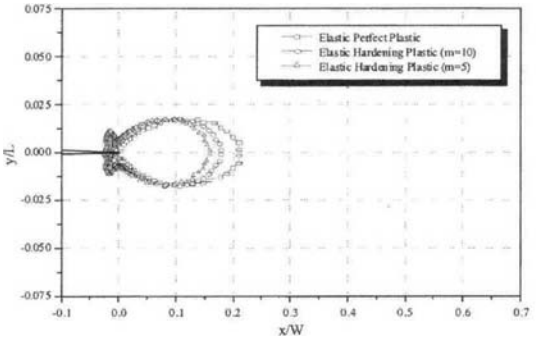

Fig. 15 The change of the plastic zone size for the various hardening exponents under Mode I (σ_0/σ_Y=0.24)

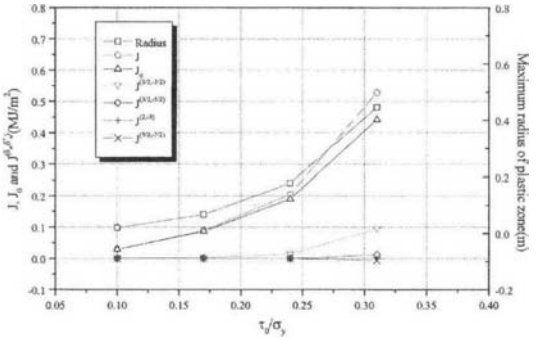

Fig. 16 The maximum radius of the plastic zone and J, J_0 and $J^{(\delta_n,\delta_n^c)}$ versus the applied Mode II loading (m=10)

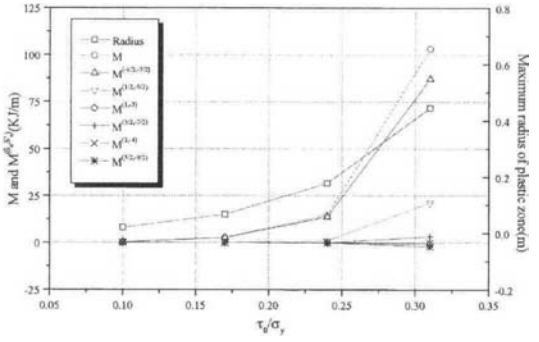

Fig. 17 The maximum radius of the plastic zone and M and $M^{(\delta_n,\delta_n^c)}$ versus the applied Mode II loading (m=10)

singularities to the J-integral toward the positive value and the increase of the difference between M and $M^{(-1/2,-3/2)}$ and between J and J_0 when the applied loading increases and as the power-law hardening exponent increases.

The plastic zone shapes of the Mode II for the variations of the applied loading and the power-law hardening exponent are shown in Fig. 14 and 15, respectively. We obtain the variation of the plastic zone size and shape as the applied loading and the power-law hardening exponent change. To show the change of the two-state J-integral, the two-state M-integral and the size of the plastic zone depending upon the change of the applied loading and the power-law hardening exponent, we plot these together with the two-state J-integrals and the two-state M-integrals associated with the higher order singularities (Fig. 16 through 19). All of these figures show that J, J_0 and each value of $J^{(\delta_n,\delta_n^c)}$ in addition to M and $M^{(\delta_n,\delta_n^c)}$ increase along with the maximum plastic zone size. Furthermore we find that $J^{(1/2,-3/2)}$ and $M^{(-1/2,-3/2)}$ are the most dominant values in all $J^{(\delta_n,\delta_n^c)}$ and $M^{(\delta_n,\delta_n^c)}$ components respectively. Furthermore $M^{(\delta_n,\delta_n^c)}$ components except for $M^{(-1/2,-3/2)}$ cancel out one another, and then the summation of the components are almost equal to difference between $M^{(-1/2,-3/2)}$ and M in Mode II, which is the case for Mode I also (Jeon and Im 2001).

Note that the term $J-J_0=\sum J^{(\delta_n,\delta_n^c)}$ represents the energetic force associated with the translation of the plastic zone with the crack tip being fixed (see Jeon and Im, 2001). Therefore this term depends upon the size and shape of the plastic zone as well as the loading and the specimen

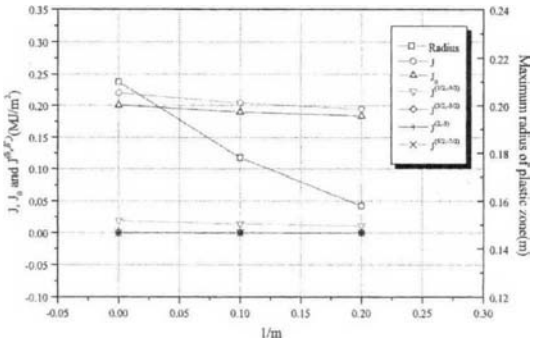

Fig. 18 The maximum radius of the plastic zone and J, J_0 and $J^{(\delta_n,\delta_n^C)}$ versus the hardening exponents under Mode II ($\tau_0/\sigma_Y=0.24$)

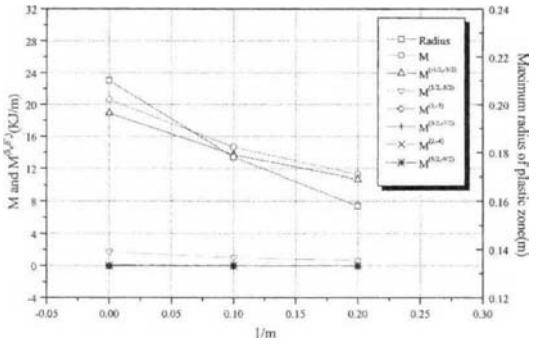

Fig. 19 The maximum radius of the plastic zone and M and $M^{(\delta_n,\delta_n^C)}$ versus the hardening exponents under Mode II ($\tau_0/\sigma_Y=0.24$)

geometry. Furthermore there may be some correlation between this term and the configuration of the plastic zone. To examine the role of the dominant eigenfields, we consider the same specimen as in Fig. 4 but with different boundary conditions in terms of displacements, which are consistent with the major eigenstates including the eigenfields of the eigenvalues $-1/2$, 0, $1/2$, Λ. Taking only the two major terms, we assume the displacements prescribed on the boundary, consistent with the following two-term expansion:

$$u_i^l=A^l r^{-1/2+1}f_i(\theta)+C^l r^{1/2+1}h_i(\theta) \quad (i=1,\ 2 \text{ and } l=1,\ 2,\ 3) \tag{17}$$

where 'i' represents the displacement components, and 'l' indicate different boundary conditions. Furthermore, $f_i(\theta)$ and $h_i(\theta)$ represent the θ-variation of the eigenfunction in Eq. (9e, f). Note that we do not consider the eigenvalue $\delta_1=0$ in

Table 8 The values of the coefficient A^l and C^l of the displacements prescribed on the boundary

δ_n	Coefficients	Case 1(l=1)	Case 2(l=2)	Case 3(l=3)
−0.5	A^l	.91970328E−03	.91970328E−03	.91970328E−03
0.5	C^l	.00000000E+00	.31090894E−03	−.31090894E−03

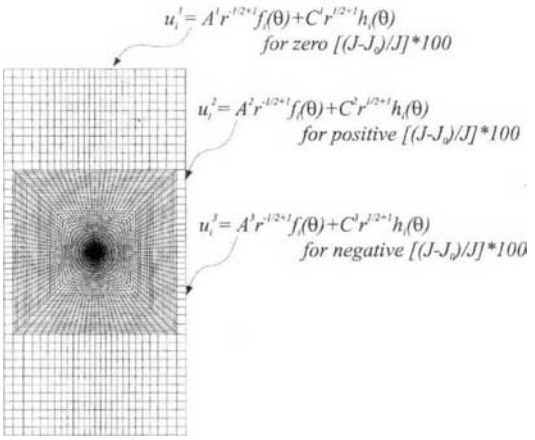

Fig. 20 The finite element mesh and displacement boundary condition under Mode II

the above displacement boundary condition because the T-stress does not exist in Mode II. To set realistic displacement boundary conditions we first solve for $\tau_0/\sigma_Y=0.24$. The resulting coefficients for $\delta_n=-1/2$ and $1/2$ are used for A^2 and C^2. We choose $A^1=A^3=A^2$, $C^1=0$, $C^3=-C^2$ (see Table 8).

The imposition of the displacements shown in Eq. (17) on the boundary will lead to exactly the same field inside the domain before a plastic zone is formed around the crack tip. Once the plastic zone appears at the tip, the second order nonsingular terms, reflected from the plastic zone, will also appear as well in addition to the higher order singular eigenfields. However, the leading order nonsingular terms will still be given by the two eigenfields prescribed. Note that the eigenfield of $\delta_2=1/2$ controls $J^{(-3/2,1/2)}$ while the eigenfield of $\delta_{-2}=-3/2$ is nothing but a field reflected from the formation of the plastic zone. Without including the eigenfield of $\delta_2=1/2$ on the exterior boundary, we are not able to take into account the leading order term of the energy

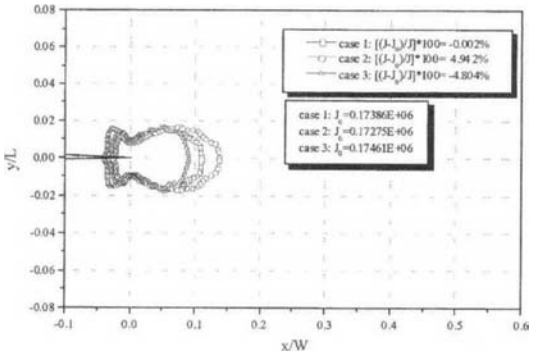

Fig. 21 The change of the plastic zone shape depending upon the sign of $[(J-J_0)/J]^*100$ under Mode II ($m=10$)

release rate associated with the translation of the plastic zone itself; we have only $J=J_0$ up to the leading order in this case. Therefore the first case $l=1$ produces almost zero value of of $[(J-J_0)/J]^*100$, and it is found that the second case ($l=2$) and the third case ($l=3$) yields a positive and negative value, respectively.

From Fig. 21 we see the apparent change of the plastic zone shape between the case of $l=2$ and the case of $l=3$ compared with the plastic zone of the case of $l=1$. All of these three cases have almost the same J_0 value, which means approximately the same energy release rate for translation of the crack tip singularity in the absence of plastic zone under Mode II. The negative value of $[(J-J_0)/J]^*100$ contracts the yield zone in the x_1-direction and slightly translate the yield zone in the negative x_1-direction, while the positive value of $[(J-J_0)/J]^*100$ expands it in the x_1-axis and tends to translate the yield zone slightly in the positive x_1-direction, compared with the plastic zone for the case of $l=1$. Thus the sign of $[(J-J_0)/J]^*100$ for Mode II, which is dominantly affected by the eigenfunction term of $\delta_2=1/2$, is related to the shape of the plastic zone. The similar correlation between the plastic zone shape and $[(J-J_0)/J]^*100$ was discussed for mode I by Jeon and Im (2001).

From the structure of $J^{(\delta_n,\delta_n^c)}$, it follows that there would be no energetic force or configurational force associated with translation of the plastic zone, i.e., zero $(J-J_0)$, if any of the higher order nonsingular eigenfields, including the term $\delta_2=1/2$, is not present on the boundary condition (16). For $J^{(1/2,-3/2)}$ will be zero in the absence of the term of $\delta_2=1/2$ regardless of the magnitude of the intensity of the higher order singularity $\delta_{-2}=-3/2$, which is generated along with the appearance of the plastic zone even if all the higher order nonsingular terms are absent from the far-field boundary. This clearly shows the limitation of some works in relation to the role of T-stress field (for examples, Betagon and Hancock, 1991; Bibly et al, 1986). The first order additional energetic force $J-J_0$ was neglected in these works because only the K-field and T-stress were considered on the external boundary of their models.

6. Conclusions

We have investigated the higher order singularities including their energetics in elastic-plastic cracks under Mode II systematically. With the aid of the eigenfunction solutions and the two-state conservation integrals as well, we have calculated the numerical results for the intensities of the higher order eigenvalues in the elastic-plastic crack under Mode II deformation. We may draw the following conclusions.

(1) The explicit formulations of the J-integral, the M-integral and the two-state conservation integrals for elastic-plastic crack problem under Mode II deformation are derived by using the complete Williams eigenfunction expansion including both positive and negative eigenvalue δ_n, in an annular region outside the plastic zone around the crack tip. The present results show that the Laurant series type expansion for mode II cracks rapidly converges in terms of the J- and M-integral even for the large scale yielding.

(2) The most dominant value of the two-state J-integrals under Mode II is computed by the eigenvalue $\delta_{-1}=-3/2$, and the associated two-state integrals $J^{(1/2,-3/2)}$ and $M^{(-1/2,-3/2)}$ constitute the major substantial portions of $\sum_{n=-1}^{-\infty} J^{(\delta_n,\delta_n^c)}$ and $\sum_{n=-2}^{-\infty} M^{(\delta_n,\delta_n^c)}$, i.e., the main contributions of the

higher order singularities to the J-integral and M-integral, respectively, under Mode II.

(3) A positive value of $[(J-J_0)/J]^*100$ tends to expand the plastic zone in the direction of the crack tip ligament while a negative value of this parameter to contract the plastic zone in the direction opposite to the crack tip ligament.

(4) A first order contribution to $J-J_0$ fails to appear if the higher order term of $\delta_2=1/2$ is not present on the boundary condition.

Acknowledgment

The present study was sponsored by the Korea Research Foundation (Grant#: 1998-018-E00049). The authors gratefully acknowledge this financial support.

References

Betagon, C. and Hancock, J. W., 1991, "Two-Parameter Characterization of Elastic-Plastic Crack-Tip Fields," *ASME J. Appl. Mech.*, Vol. 58, pp. 104~110.

Bibly, B. A., Cardew, G. E., Goldethorpe, M. R. and Howard, I. C., 1986, "A Finite Lement Investigation of the Effects of Specimen Geometry on the Fields of Stress and Strain at the Tips of Stationary Cracks," *Size Effects in Fracture I*, pp. 37~46.

Chen, F. H. K. and Shield, R. T., 1977, "Conservation Laws in Elasticity of the J-Integral Type," *Z. Angw. Math. Phys. (ZAMP)*, Vol. 28, pp. 1~22.

Chen, Y. H. and Hasebe, N., 1994a, "Further Investigation of Comninou's EEF for an Interface Crack With Completely Closed Faces," *Int. J. Engng Sci.*, Vol. 32, pp. 1037~1046.

Chen, Y. Z. and Hasebe, N., 1994b, "Eigenfunction Expansion and Higher Order Weight Fuctions of Interface Cracks," *ASME J. Appl. Mech.*, Vol. 61, pp. 843~849.

Chen, Y. H. and Hasebe, N., 1997, "Explicit Formulation of the J-Integral Considering Higher Order Singular Terms in Eigenfunction Expansion Forms. Part I. Analytical Treatments," *Int. J. Fract.*, Vol. 85, pp. 11~34.

Cho, Y. J., Beom, H. G. and Earmme, Y. Y., 1994, "Application of a Conservation Integral to an Interface Crack Interacting with Singularities," *Int. J. Fract.*, Vol. 65, pp. 63~73.

Choi, N. Y. and Earmme, Y. Y., 1992, "Evaluation of Stress Intensity Factors in a Circular Arc-shaped Interfacial Crack using L-integral," *Mech. Materials*, Vol. 14, pp. 141~153.

Eshelby, J. D., 1956, "The Continuum Theory of Lattice Defects," *Solid State Phisics*, Vol. III, pp. 79~144.

Hui, C. Y. and Ruina, A., 1995, "Why K? High Order Singularities and Small Scale Yielding," *Int. J. Fract.*, Vol. 72, pp. 97~120.

Im, S. and Kim, K. S., 2000, "An Application of Two-State M-Integral for Computing the Intensity of the Singular Near-Tip Field for a Generic Wedge," *J. Mech. Phys. Solids*, Vol. 48, pp. 129~151.

Jeon, I., Cha, B. W. and Im, S., 1996, "Edge Delamination in a Laminated Composite Strip Under Generalized Plane Deformations," *Int. J. Fract.*, Vol. 77, pp. 95~110.

Jeon, I. and Im, S., 2001, "The Role of Higher Order Eigenfields in Elastic-Plastic Cracks," *J. Mech. and Phys. Solids*, Vol. 49, pp. 2789~2819.

Kfouri, A. P., 1986, "Some Evaluation of Elastic T- Term Using Eshelby's Method," *Int. J. Fract.*, Vol. 30, pp. 301~315.

Kim, Y. J. and Lee, H. Y., "Decomposition of Interfacial Crack Driving Forces in Dissimilar Joints," *KSME Int. J.*, Vol. 14, pp. 30~38.

Knowles, J. K. and Sternberg, E., 1972, "On a Class of Conservation Laws in a Linearized and Finite Elastostatics," *Arch. Rat. Mech. Anal.*, Vol. 44, pp. 187~211.

Li, F. Z., Shih, C. F. and Needleman, A., 1985, "A Comparison of Methods for Calculating Energy Release Rates," *Engr. Fract. Mech.*, Vol. 21, pp. 401~421.

Matos, P. P. L., McMeeking, R. M., Charalambides, P. G. and Drory, M. D., 1989, "A Method for Calculating Stress Intensities in Bimaterial Fracture," *Int. J. Fract.*, Vol. 40, pp. 235~254.

McMeeking, R. M., 1977, "Finite Deformation Analysis of Crack-Tip Opening in Elastic-Plastic Materials and Implications for Fracture," *J.*

Mech. and Phys. Solids, Vol. 25, pp. 357~381.

Rice, J. R., 1968, "A Path Independent Integral and the Approximate Analysis of Strain Concentration by Notches and Cracks," *ASME J. Appl. Mech.*, Vol. 35, pp. 379~386.

Timoshenko, S. P. and Goodier, J. N., 1987, "Theory of Elasticity," *Mcgraw-Hill International Editions* (3rd Edition).